RADIOCARBON, Vol 53, Nr 2, 2011, p 345–357

USING THE ^{14}C BOMB PULSE TO DATE YOUNG SPELEOTHEMS

Ed Hodge[1] • Janece McDonald[2,3] • Matthew Fischer[1] • Dale Redwood[2] • Quan Hua[1] • Vladimir Levchenko[1] • Russell Drysdale[4] • Chris Waring[1] • David Fink[1]

ABSTRACT. Three modern speleothems were sampled at high resolution for radiocarbon analysis to identify their bomb-pulse signatures and to construct chronologies. Each speleothem exhibited a different ^{14}C response, presumed to be related to site characteristics such as vegetation, temperature, rainfall, depth below the surface, and water pathway through the aquifer. Peak ^{14}C activity for WM4 is 134.1 pMC, the highest cited thus far in the literature and suggestive of a lower inertia at this site. Dead carbon fractions for each stalagmite were calculated and found to be relatively similar for the 3 speleothems and lower than those derived from Northern Hemisphere speleothems. An inverse modeling technique based on the work of Genty and Massault (1999) was used to estimate soil carbon residence times. For each speleothem, mean soil ^{14}C reservoir ages differed greatly between the 3 sites, ranging from 2–6.5 to 32–46 yr.

INTRODUCTION

The ability to construct a robust chronology for young (<100 yr old) speleothems (cave carbonate deposits including stalagmites, stalactites, and flowstone) is highly desirable as it allows for the comparison and calibration of speleothem geochemical proxies (e.g. trace elements and stable isotopes) with instrumental climate records. Speleothems can provide high-resolution climate records in areas where other archives are not available, poorly preserved, and/or difficult to date. This situation exists for most parts of Australia.

Speleothems are most commonly and successfully dated using uranium-series techniques because they incorporate uranium during deposition, tend to behave as closed systems, and often include very little detrital contamination (Richards and Dorale 2003). However, in young samples (i.e. <200–300 yr old), Th/U ages can be very imprecise due to insufficient ingrowth of ^{230}Th, particularly where uranium concentrations are low (<1 $\mu g\ g^{-1}$). While ^{210}Pb has been used to date young speleothems (Baskaran and Illiffe 1993), lead (Pb) concentration can be variable and large samples are required (>1 g), which precludes a high-resolution chronology for most speleothems. Occasionally, speleothems have laminations, comprising either visible or luminescent, and/or trace element cycles (Baker et al. 1993; Genty and Quinif 1996; Roberts et al. 1998), but without an independent chronology it is difficult to verify whether these are annual.

While conventional ^{14}C dating may be imprecise for samples <300 yr old due to large fluctuations in atmospheric ^{14}C for the period AD 1650–1950 (Geyh 2005; Hua 2009), the presence of a huge increase of atmospheric ^{14}C during the nuclear weapons testing of the 1950–60s provides a chronostratigraphic framework for the dating of young speleothems. The ^{14}C bomb pulse has been measured in a number of speleothems previously (Genty and Massault 1997, 1999; Genty et al. 1998), but in these cases it has involved investigating the carbon cycle using annually banded samples rather than for chronological purposes. By undertaking high-precision accelerator mass spectrometry (AMS) ^{14}C analysis on small subsamples, a detailed bomb-pulse profile may be obtained, allowing the assignment of a chronology since ~1950 and inverse modeling of ^{14}C uptake by the speleothem. This technique has proven successful in matching a 56-yr speleothem $\delta^{18}O$ record with the instrumental rainfall record from Gibraltar (Mattey et al. 2008); the methods used here are described in detail in that paper.

[1]Australian Nuclear Science and Technology Organisation (ANSTO), Kirrawee DC, NSW 2232, Australia.
[2]Environmental and Climate Change Research Group, University of Newcastle, Callaghan, NSW 2308, Australia.
[3]Corresponding author: Email: janece.mcdonald@newcastle.edu.au.
[4]Department of Resource Management and Geography, University of Melbourne, Victoria 3010, Australia.

The bomb-pulse chronologies of 3 Australian stalagmites are presented. There is great interest in reconstructing rainfall histories in this region because local water supplies for major cities and agriculture are greatly influenced by irregular drought cycles linked to variability in the El Niño Southern Oscillation (ENSO), Interdecadal Pacific Oscillation (IPO), Indian Ocean Dipole (IOD), and Southern Annular Mode (SAM) cycles (Verdon-Kidd and Kiem 2009), and potentially by long-term climate change. To help interpret relative contributions of these climate phenomena, as well as the magnitude and frequency of extreme events, robust chronologies are essential.

SAMPLE DESCRIPTIONS AND BACKGROUND

SC4

Smiths Cave (10°30′S, 105°34′E), located on the north coast of Christmas Island, Indian Ocean, is a shallow cave system (~20–30 m) formed in Late Tertiary to Quaternary age limestone. Present-day average precipitation is 2154 mm/yr, humidity is 80–90%, and mean temperatures vary between 22.5 and 27.8 °C. Vegetation above the cave consists mainly of open, semi-deciduous rainforest developed on shallow terra rossa soils. Sample SC4 (Figure 1A) was recovered ~150 m from the entrance in November 2004. SC4 is a ~196-mm stalagmite composed of porous, white/yellow crystalline calcite. SC4 was active at time of recovery, and it is believed that deposition was continuous throughout formation. There are visible laminations comprising dark and light bands, with approximately 800 couplets along the growth axis, which are thought to be annual but not yet confirmed.

WM4

The Wombeyan Caves (34°19′S, 149°59′E) are located on a dissected plateau east of the Great Dividing Range, ~125 km SW of Sydney. The Wombeyan karst comprises a NE/SW trending belt of marble ~200 m thick and composed of a single unit (Wombeyan Marble) of relatively uniform geochemical composition. The soils above the caves are primarily eolian derived (McDonald 2005), typically very thin (<4 cm depth), and consist of marble fragments, fine gravel, dark brown humic matter, and red silty clay (Jennings et al. 1982). Approximately 50% of the landscape is occupied by exposed bedrock. The vegetation is open woodland, comprising randomly spaced native evergreen trees with an understory of shrubs, forbs, and grasses. The region's annual rainfall is highly variable (mean annual precipitation = 848 mm; coefficient of variation = 26.1%). Mean summer maximum precipitation exceeds the mean winter minimum precipitation by ~30%. High summer temperatures (mean January maximum = 27.5 °C) produce high evaporation rates and hence reduced recharge to the caves. Conversely in winter, lower temperatures (mean July maximum = 10.1 °C) result in higher effective rainfall amounts. Stalagmite WM4 (Figure 1B) was an active stalagmite at the time of its collection in May 2005. It was growing onto flowstone in Mulwaree Cave at a depth of ~20 m below the surface. It is 93 mm high and has a diameter of approximately 49 mm. It has precipitated from a fast-discharge drip, which has been shown to record the site hydrology by changes in its hydrochemistry (J McDonald, unpublished data).

JWT-1

The Jenolan Caves (33°49.14′S, 150°117.2′E) are located ~110 km west of Sydney and consist of a number of interconnected caves formed in Silurian limestone, many of which are open to the public. Present-day average precipitation is 946 mm/yr and mean annual aboveground temperature is 11.4 °C. Vegetation above the caves consists of moderately dense eucalypt forest with relatively thin overlying soils (<1 m). Sample JWT-1 was recovered from the northern end of River Cave at a depth of ~200 m below the surface. JWT-1 (Figure 1C) is part of a calcite shawl stalactite that grew on a

galvanized steel wire, erected in AD 1938. In August 1998, the wire broke and a section of the shawl was donated by the Jenolan Caves Reserve Trust. JWT-1 is ~63 mm long, 8–10 mm thick, and composed of dense, white to gray crystalline calcite. The growing surface consists of vertical dog-tooth crystals. Water flowed along the leading edge of the shawl, depositing calcite from a thin film, and it is believed deposition was continuous until the wire broke.

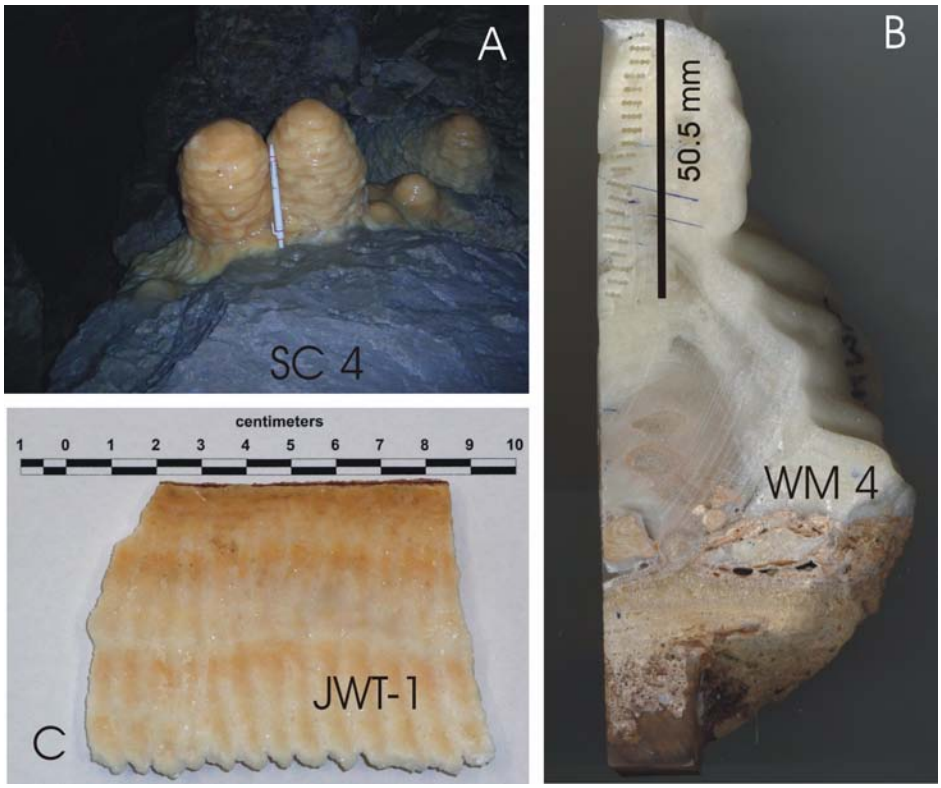

Figure 1 A, B, and C are images of the speleothems that are discussed in this study. (A) is SC4, a 196-mm stalagmite from Christmas Island; (B) is WM4 and shows the ^{14}C sampling points at 250-µm intervals. JWT-1 (C) is part of a shawl that grew along a piece of wire.

METHODS AND RESULTS

Sample Preparation

All samples were cut to size and a section of the central axis exposed for subsampling. Slices were cleaned thoroughly before milling or drilling. Powders from SC4 and JWT-1 were milled for AMS ^{14}C analysis using a Micromill 2000 LE-ER system and a 0.5-mm tungsten carbide milling bit using a micromilling method developed at the Research School of Earth Sciences, The Australian National University (Gagan et al. 1994). WM4 was drilled at discrete intervals using a 1.0-mm-diameter tungsten carbide drill bit. JWT-1 was continuously milled at 1-mm intervals yielding 63 powder samples, each weighing ~20 mg. WM4 was drilled at 2.5-mm intervals from the tip and yielded 20 powder samples, each weighing around 10 mg. SC4 produced 60 samples at 200-µm intervals, each around 10 mg in weight, based on continuous milling from the outer growth surface.

For AMS ^{14}C analysis, ~8 mg of speleothem calcite powder was dissolved in 2 mL 85% H_3PO_4 and the evolved CO_2 converted to graphite using H_2 and Fe catalysts. The graphite was rear-pressed into a 1.60-mm-diameter recess in aluminium cathodes for AMS measurement. The technical aspects of these methods are described in Hua et al. (2001).

AMS ^{14}C Measurement

^{14}C was measured on the 2MV HVEE "STAR" accelerator in the Institute for Environmental Research, ANSTO (Fink et al. 2004). Cathodes were generally measured for ~30 min in total, giving around 80,000 counts of ^{14}C and a statistical uncertainty <0.4%. Interspersed were measurements of oxalic acid I and II (HOxI and HOxII) normalization standards, IAEA C1 marble procedural blank, and unprocessed commercial graphite (spectroscopic-grade powdered graphite from Union Carbide Co.) for assessing machine background (>55,000 yr). As the samples are modern with a pMC (percent modern carbon) >90%, neither of the blank corrections was significant in altering final values. $\delta^{13}C$ for correction of the $^{14}C/^{12}C$ ratio was measured on portions of the same graphite using a Micromass IsoPrime elemental analyzer/isotope ratio mass spectrometer (EA/IRMS).

Radiocarbon Activity

The bomb-pulse profiles from the 3 speleothems (Figure 2) show the same overall pattern but display different amplitudes of ^{14}C activity response to the atmospheric ^{14}C pulse. The speleothems have pre-bomb values (on the left of Figure 2, before the sharp rise in pMC) between 90–95 pMC and final values between 108–111 pMC, although times of collection differ slightly, with JWT-1 collected in 1998, WM4 in 2005, and SC4 in 2004. Peak values vary between speleothems, with JWT-1 the lowest at 112.6 ± 0.6 pMC, SC4 at 119.5 ± 0.5 pMC, and WM4 the highest at 134.1 ± 0.6 pMC. Peak activity for JWT-1 is similar to that measured in some European speleothems (Genty and Massault 1999), with SC4 peak activity being slightly higher, and WM4 peak activity the highest of any in the currently published literature.

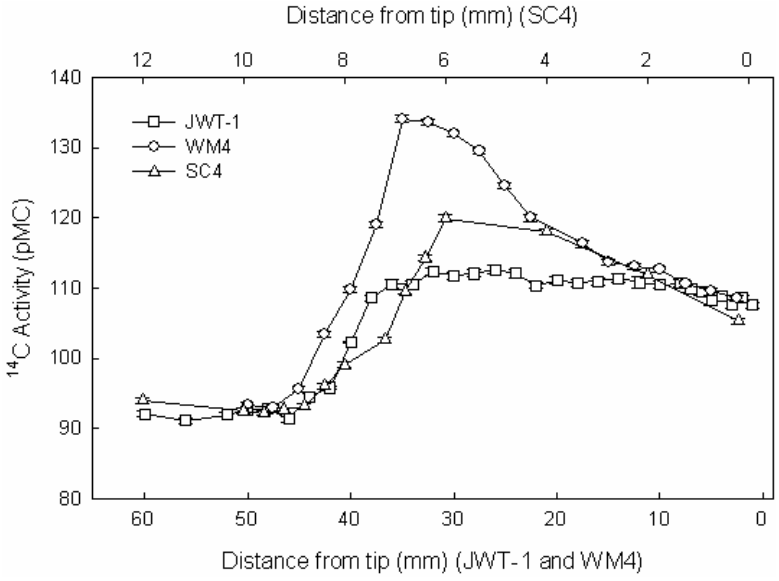

Figure 2 Speleothem ^{14}C activity plotted against distance from tip, where the lower *x* axis is for JWT-1 and WM4, and upper *x* axis for SC4. Error bars are 1 σ.

Dead Carbon Fraction (DCF)

The dead carbon fraction (DCF) is the ratio between the measured ^{14}C concentration (i.e. pMC) in the speleothem and the atmospheric ^{14}C concentration at a particular time. Effectively, DCF is equivalent to the proportion of carbon incorporated into the speleothem from limestone bedrock and ancient soil organic matter (SOM), assuming these sources contribute negligible ^{14}C. The best reference point from which to estimate the long-term DCF in young speleothems is in the immediate pre-bomb period (~1950–1954) before atmospheric and short-term soil ^{14}C reservoirs are perturbed by bomb ^{14}C, and when atmospheric and speleothem ^{14}C activity should be relatively constant (Genty et al. 1999). This DCF can be calculated using the following:

$$DCF = \left[1 - \left(\frac{a^{14}C_{spel}}{a^{14}C_{atm}}\right)\right] \times 100\,\% \quad (1)$$

where $a^{14}C_{spel}$ is the measured pre-bomb speleothem ^{14}C activity and $a^{14}C_{atm}$ the average pre-bomb Southern Hemisphere atmospheric ^{14}C activity between 1950–1954 measured on tree rings from Tasmania and Armidale, Australia (Hua et al. 2000, 2003) and Chile (Stuiver and Brazuinas 1998), and atmospheric CO_2 samples from Pretoria (Vogel and Marais 1971). The error in the DCF is calculated by integrating the average error of the pre-bomb atmospheric ^{14}C activity (1950–1954), which is 0.27 pMC, and the average error in AMS measurements of pre-bomb speleothem ^{14}C activity, which is 0.4 pMC for each sample. Estimated DCF values (expressed as %) are relatively similar for the 3 speleothems: JWT-1 = 6.1 ± 0.4; SC4 = 5.1 ± 0.4; WM4 = 5.0 ± 0.4.

Estimating a Chronology

By comparing the shape of our ^{14}C activity profiles with atmospheric ^{14}C changes, and utilizing findings from previous bomb-pulse speleothem studies and pre-existing information such as start or collection date, a chronology for each speleothem can be constructed.

The shawl (JWT-1) started growing in 1938 and was collected in 1998, although we actually assign the date of 1940 to the oldest data point as it is assumed that nucleation and commencement of growth may have taken 1–2 yr after the wire was erected (J McDonald, unpublished data). Some contemporary ^{14}C is always incorporated into a speleothem, even if diluted by carbon from slower pathways, so the start of the rising limb of the bomb-pulse should not lag by more than 1–2 yr behind the start of the rise in atmospheric ^{14}C activity in 1955 (Genty and Massault 1999). In JWT-1, therefore, we assign the point just before the start of the rapid rise in ^{14}C activity to 1955. Assuming the inertial effect (the lag between peak atmospheric ^{14}C activity and peak speleothem ^{14}C activity) will be roughly similar for speleothems with similar peak ^{14}C activity values (Genty and Massault 1999), the lag of JWT-1 peak ^{14}C activity is likely to be around 15 yr after 1964, so this point is assigned to 1979. The resultant chronology (Figure 3) shows that the extension rate for the analyzed section of JWT-1 was likely to have been slower initially, then faster towards the end. This probably has more to do with growth form/behavior of the shawl than climate since the younger (higher extension rate) interval was drier compared to the middle 1900s, so slower recent growth would be expected.

For SC4, the first point (the tip of the stalagmite) should be late 2004, when it was collected. A penultimate age of 1955 can be assigned to the immediate pre-bomb sample. The peak value is higher than JWT-1, at 119.5 pMC, and therefore is likely to reflect a lower inertia (Genty and Massault 1999) and may be assigned to 1972. The last point is difficult to assign with any precision but may be around 1950, making the resultant chronology linear (Figure 3). The choice of these ages

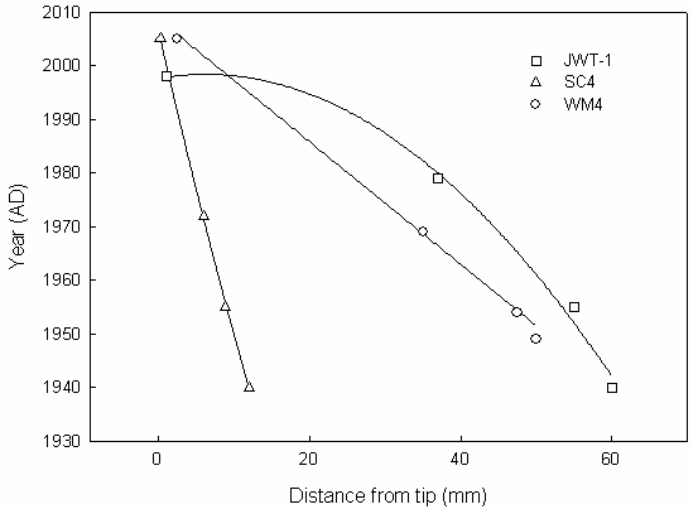

Figure 3 Polynomial regression lines representing age-depth models used for preliminary chronology.

is supported by the nearly equally spaced visible laminae, which are likely to represent annual increments and uniform growth rate.

The tip of WM4 is assigned to 2005, the year of collection. As the peak value is very high (134.1 pMC), it can be reasonably assumed that it has a lower inertia than either SC4 or JWT-1, but must be younger than the peak in atmospheric ^{14}C activity in 1966 (Hua and Barbetti 2004), and thus the peak value is assigned an age of 1969. The penultimate data point is just before the increase at the start of the bomb-pulse and therefore assigned the age of 1954. The final point is unlikely to be much more than 5 yr older than this unless the growth rate was markedly slower in this part of the stalagmite. As there are no obvious textural changes over this part of the sample, the last point is assigned the date of 1949 based on the ensuing modeled chronology, which is linear (Figure 3).

The resultant bomb pulse profiles (Figure 4) therefore show different responses to the increase in atmospheric ^{14}C activity. WM4 responds rapidly and has a peak ^{14}C activity only ~30 pMC lower than the Southern Hemisphere atmosphere. It then declines rapidly after the peak, with ^{14}C activity similar to the atmosphere in the early 1990s. SC4 does not increase as rapidly as WM4, reaching peak ^{14}C activity later and with a lower value but by the mid-1990s had fallen to similar values as WM4 and the atmosphere. JWT-1 appears to respond as rapidly to the start of the bomb pulse as WM4 but after ~1962 ^{14}C activity starts to level out and the final ~2 pMC increase takes almost 18 yr, with peak ^{14}C activity occurring in 1979. After this point, JWT-1 undergoes a slow decline in ^{14}C activity, remaining below the other 2 speleothems and atmospheric ^{14}C values until the end of growth in 1998.

Inverse Modeling of Soil Organic Matter

Here, we use the ^{14}C activity measurements and the estimated chronology to model soil carbon residence times over the bomb-pulse period. The Appendix describes a forward model for ^{14}C in speleothems, based on Genty and Massault (1999). The initial equation in that model is re-expressed here as:

$$pM_{soil} = (pM_{Y1}e^{p1} + pM_{Y2}e^{p2} + pM_{Y3})(1 + e^{p1} + e^{p2})^{-1} \quad (2)$$

where pM_{soil} and pM_{Yi} (in pMC) are the ^{14}C content of the soil atmosphere (CO_2) and mean atmospheric CO_2, respectively. Model 1 is derived solely from the isotope mass balance constraint. The model has 5 free parameters ($Y1$, $Y2$, $Y3$, $p1$, $p2$). $Y1$, $Y2$, and $Y3$ are the number of years over which each "soil carbon reservoir" averages atmospheric ^{14}C. Parameters $p1$ and $p2$ help force the "sum to unity" constraint on the reservoir mixing coefficients (e.g. in the above formulation, if $p1 = p2 = 0$, then the mixing coefficients = 1/3).

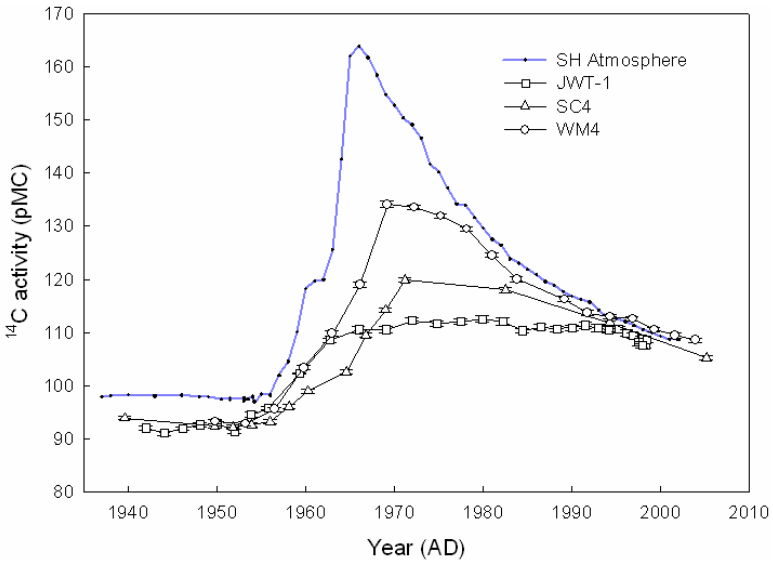

Figure 4 Speleothem ^{14}C activity plotted using preliminary chronologies, against Southern Hemisphere (SH) atmospheric ^{14}C activity. Error bars are 1 σ. Pre-bomb (1936–1954) SH atmospheric ^{14}C activity comprises averaged tree-ring data from Tasmania and Chile (Stuiver and Braziunas 1998), Tasmania (Hua et al. 2000), and Armidale, Australia (Hua et al. 2003) and atmospheric measurements from Pretoria (Vogel and Marais 1971). Post-bomb (1955 onwards) SH atmospheric ^{14}C activity comprises atmospheric data compiled by Hua and Barbetti (2004) for 1955–1997 and unpublished update data for 1998–2002.

Model 1 assumes that there are 3 reservoirs of soil organic matter that contribute ^{14}C to the soil atmosphere. Each reservoir has an impulse response function which uniformly weights the contribution of pM_{atm} at time (t–τ) to give the present reservoir pM at time t. The pMC from the 3 reservoirs is then mixed in some proportion. Model parameter estimation is discussed in the next section.

The ^{14}C activity of the limestone bedrock is assumed to be 0. Although there are fractionation effects (Appendix 1) between the pM_{soil} and pM_{aq} (dissolved carbon), and between pM_{aq} and pM_{SP} (speleothem), the total variance of these fractionation effects is very small compared to the variance of pM_{soil}. The result of this is that over the period 1940–2000, the shape of pM_{SP} curve is entirely determined by the shape of the pM_{soil} curve. The pM_{SP} is simply offset from pM_{soil} by the fractionation effects and the dcp (see Appendix). This relationship is used to our advantage in the estimation of the model's parameters.

Parameter Estimation

Parameter estimation for the above models requires knowing pM_{atm} (the model input) and pM_{SP} (the model output). For pM_{atm}, we use the updated Southern Hemisphere atmospheric ^{14}C data set of Hua and Barbetti (2004), while pM_{SP} from the 3 speleothems is as described previously.

Owing to the structure of the above model, it is easier to invert the model using a 2-step process, rather than estimating all the parameters simultaneously. In Step 1, $Y1$, $Y2$, and $Y3$ are "estimated." These parameters are estimated subject to the following constraints: $1<Y1<20$, $20<Y2<50$, $50<Y3<150$. These values are based on the idea of soil carbon reservoirs with fast, medium, and slow turnover. The pM_{atm} curve is first smoothed over 2, 3, …, 150 yr, providing a matrix with all possible $Y1$, $Y2$, $Y3$ curves. Then, all possible combinations of $Y1$, $Y2$, and $Y3$ are sampled sequentially from this matrix, under the constraints given above (e.g. $1<Y1<20$). In Step 2, an optimization algorithm is employed to find $p1$ and $p2$, using the objective function $Corr$ (pM_{soil}, pM_{SP}) (i.e. Pearson's squared correlation coefficient between pM_{soil} and pM_{SP}). Using the correlation coefficient takes advantage of the fact that the shapes of the pM_{soil} and pM_{SP} should be similar, and as a result there are fewer parameters that need to be optimized. The parameters $p1$ and $p2$ do not need to be constrained in anyway, so the optimization can be performed using any unconstrained optimization method (e.g. Press et al. 2007). By looping through all the possible combinations for $Y1$, $Y2$, $Y3$, and then optimizing for $p1$ and $p2$, the absolute "best-fitting" $p1$, $p2$ values are found for all $Y1$, $Y2$, $Y3$ combinations.

The overall results are presented in Table 1 and show that soils above JWT-1 have a mean SOM residence time of 32–46 yr, 15–18 yr above SC4 and 2–6.5 yr above WM4 (Table 1). These differ from the results obtained using the model of Genty and Massault (1999), with our model results displaying much faster SOM turnover times, particularly for WM4 and SC4 (Table 1), a point which we discuss below.

DISCUSSION

The results presented here represent a significant addition to the limited information currently available on Southern Hemisphere speleothem and soil carbon dynamics, and provide an important basic chronology whereby these speleothems may be compared with the recent instrumental climate record. Here, we compare the findings between the 3 records we have obtained from Australia, and against results from the published literature. In addition, we evaluate our method of establishing a chronology and estimating SOM reservoir residence times.

Dead Carbon Fraction

The dead carbon fractions (DCFs) of the 3 speleothems in this study are relatively low, between 5.0 and 6.1% (Table 1). Apparent DCFs calculated using the same method of measuring pre-bomb ^{14}C activities in speleothems from caves in France, Belgium, and Slovenia range from 9% to 11.6% (Genty and Massault 1999). Average DCFs for a larger number of speleothems from northern Europe range from 9–17.5 ± 1.5% (Genty et al. 2001). Our low DCFs therefore appear to be an exception to the published values. DCFs in speleothems are thought to be closely related to temperature and soil pCO_2, with vegetation type being largely responsible for the final DCF value (Genty and Massault 1999). Higher DCFs tend to occur under temperate mixed forests and lower DCFs under grassland (Genty et al. 1999, 2001). However, different vegetation and climate regimes occur at the sites in this study. In all of our sites, year-round vegetation exists that might account for faster overturning of SOM, and temperatures are generally higher than the European sites, with the exception of La Faurie Cave (Table 1). Evergreen vegetation, large areas of exposed bedrock, and thin soils (0–50 cm) may be factors causing the lowest DCF of 5.0 ± 0.4% recorded by WM4. Above this cave, carbonate dissolution and even secondary calcite dissolution (Genty and Massault 1997) must be at a minimum and coupled with a very fast SOM turnover rate, thus reducing the input of older organic matter (Genty et al. 1998). Minimum calcite dissolution will occur during short water/calcite residence times, i.e. during periods of high filtration or wet phases and the expectation is that

Table 1 Present-day environmental characteristics, ^{14}C activities, and modeled SOM components for Australian speleothems (this study), compared with European speleothems (Genty and Massault 1999): * Date of maximum ^{14}C activity in Australian speleothems is based on modeled chronology. # Using 3-component model of Genty and Massault (1999). ** Using inverse model described in this paper.

Stalagmite name	Location	Vegetation type	Mean annual preci. (mm)	Mean annual temp (°C)	Pre-bomb ^{14}C activity (pMC)	Apparent DCF (pre-bomb) %	Max ^{14}C activity (pMC)	Date of max ^{14}C activity*	Fast SOM component#	Slow SOM component#	Very slow SOM component#	Modeled mean SOM residence times**
JWT-1	Jenolan Caves, SE Australia	Semi-dense Eucalypt forest	946	11.4	92.0 ± 0.4	6.1 ± 0.4	112.6 ± 0.6	1980	C1 = 32%, Y1 = 2 yr		C3 = 68%, Y3 = 57 yr	32–46 yr
WM4	Wombeyan Caves, SE Australia	Open woodland and 50% exposed bedrock	848	12.0	93.1 ± 0.4	5.0 ± 0.4	134.1 ± 0.6	1969	C1 = 65%, Y1 = 3 yr	C2 = 35%, Y2 = 28 yr		2–6.5 yr
SC4	Smiths Cave, Christmas Island, Indian Ocean	Open, semi-deciduous rainforest	2154	25.0	93.0 ± 0.4	5.1 ± 0.4	119.5 ± 0.5	1971	C1 = 39%, Y1 = 18 yr	C2 = 29%, Y2 = 31 yr	C3 = 32%, Y3 =104yr	15–18 yr
Fau-stm14	La Faurie Cave, France	Grassland	860	12.9	91.0 ± 0.5	9.0 ± 1.5	113.9 ± 0.6	1980	C1 = 10%, Y1 = 5 yr	C2 = 32%, Y2 = 22 yr	C3 =58%, Y3 =130 yr	
Han-stm5	Han-sur-Lesse Cave, Belgium	Deciduous woodland	790	8.9	87.8 ± 0.7	11.2 ± 1.5	101.1 ± 0.8	1990	C1 = 12%, Y1 = 10 yr		C3 =88%, Y3 =100 yr	

although DCF values are seasonally variable, they may have a relatively uniform annual value. The DCF values for JWT-1 and WM4 are much lower than those for Fau-stm14, despite lower mean temperatures at the Australian sites, indicating that temperature is not the dominant factor. Vegetation type along with seasonality (temperature ranges and precipitation) may also play an important role at these sites.

Evaluating the Chronology

Assignment of a chronology using the ^{14}C bomb pulse may be a powerful tool for calibrating speleothem response to the instrumental climate record, but should be subjected to evaluation. In the case of the studies of Genty and Massault (1997, 1999) and Genty et al. (1998), annual laminations or dated marker horizons allowed the estimation of an independent chronology. With our speleothems, we did not have these benefits, but careful analysis of ^{14}C activity trends allowed chronologies to be assigned. In each case, we knew when the speleothem ceased growing, providing the final definitive point. Also, due to relatively high-resolution sampling we could assign the point of transition from pre-bomb to rising-limb ^{14}C activity to 1954–55 with confidence. In the case of JWT-1, we know the start of growth (1938), which provides another important marker point. The assignment of a date for peak ^{14}C activity remains the most speculative. The relationship between dampening (peak ^{14}C – pre-bomb ^{14}C relative to atmosphere) and inertia (time lag between atmospheric ^{14}C and speleothem ^{14}C peak) proposed by Genty and Massault (1999) does not hold for WM4 and therefore may be unreliable for our other samples, particularly as they all display very similar pre-bomb ^{14}C activities. The peak ^{14}C activity dates for our samples were therefore assigned by studying peak dates for the European speleothems in relation to absolute maximum ^{14}C activity and also by looking at the effects on our age-distance plots (Figure 3). The position of peak ^{14}C activity for each speleothem is within the limits of plausible growth rate variations over that time. Large-scale vegetation change has not taken place at any of the sites since the early 1900s. In addition, SC4 has visible banding, thought to be annual, which does not show a change in spacing over the period analyzed here. At present, this technique represents the best way of obtaining a chronology for young speleothems (<60 yr), and despite some uncertainty offers a better precision than U-Th or ^{210}Pb ages. Using AMS techniques, it can also be routinely undertaken on very small subsamples (1–10 mg carbonate or less) and therefore allows construction of recent growth history for quite slow-growing speleothems. This is a clear advantage in tourist show caves where larger specimens can be conserved and smaller stalagmites, often growing on man-made infrastructure, may be utilized.

SOM Reservoir Age Assessment

An important additional benefit to measuring ^{14}C in young speleothems is the information about soil carbon dynamics and carbonate dissolution rates that may be obtained. The implications of better understanding these processes and rates are clear when using speleothems from the same cave for paleoclimatic reconstruction. Using our inverse model, the mean soil ^{14}C reservoir ages differ greatly between our 3 sites, from 2–6.5 yr for WM4 to 32–46 yr for JWT-1 (Table 1). Despite similar factors affecting both, DCF variations are not so marked, although the same order is retained, with WM4 having the lowest DCF and mean soil reservoir age and JWT-1 the highest.

Factors thought to be important in the speed of SOM turnover, and therefore ^{14}C residence times, are vegetation type and climate, with the added factor of water mixing in the vadose zone of deep caves (Genty and Massault 1999). JWT-1 comes from a particularly deep passage at about –200 m and therefore water mixing may cause the much longer apparent soil carbon reservoir time than for WM4, which has a very similar climate, but only has ~20-m overlying rock thickness. The denser vegetation at Jenolan Caves may also cause slower SOM turnover, adding to this offset. The SOM

reservoir time of SC4 falls between WM4 and JWT-1, yet Christmas Island has much higher precipitation and temperature than either Wombeyan or Jenolan, and SC4 comes from a similar depth cave as WM4. On Christmas Island, vegetation type and seasonality of precipitation may be the crucial factors in determining SOM degradation rates, even though theoretically SOM turnover should be faster in a tropical environment than in temperate climate zones (Trumbore 1993). Clearly, the prediction of SOM turnover rates cannot be easily undertaken based on a few basic parameters such as vegetation type and climate. Seasonality, rock thickness, and the karst architecture may have a major effect. Drip water percolation pathways can vary significantly due to bedrock depth, lithology, and the relative proportion of fast and diffuse flow paths (Tooth and Fairchild 2003). There is also a difference between speleothems growing in the climatic and vegetation zones we have sampled and those from northern Europe, as the maximum SOM residence in Australia is 32–46 yr for JWT-1, but the European speleothems have >50% SOM reservoirs over 100 yr (Table 1) (Genty and Massault 1999). This may be partly due to differences in the models used, but may also be a real difference due to the seasonality of precipitation (European winter rainfall versus summer rainfall at these Australian sites), lower soil moisture levels leading to enhanced oxidation, and the presence of evergreen vegetation at all these Australian sites. When the ^{14}C activity profiles are modeled using the 3-reservoir model of Genty and Massault (1999), we still see a large component of the signal from each Australian speleothem made up of short residence SOM reservoirs (Table 1). However, a wider sample base from both regions is needed to verify these conclusions.

CONCLUSIONS

The first major implication of this study is that speleothems from locations with rapid SOM turnover may be most suitable for the use of this dating method because the high rate of ^{14}C activity change over the bomb pulse will allow the most accurate positioning of the chronology. The second major implication is that speleothems that come from caves with rapid SOM turnover, as indicated by high peak ^{14}C activity over the bomb pulse, are also more likely to have a rapid and less ambiguous response to other geochemical inputs. For instance, low soil residence times and less water mixing in the unsaturated zone will mean a $\delta^{13}C$ signal sensitive to external factors such as vegetation changes. Less water mixing in shallow caves also means clearer climate signals from $\delta^{18}O$ and trace elements such as Mg/Ca, which may give good indications of past rainfall amount and paleorecharge, respectively (e.g. McDermott 2004; Fairchild et al. 2006). Additionally, a rapid and perhaps seasonal response of these geochemical indicators may help further improve the chronology by allowing the counting of annual or seasonal bands. These can only be presumed annual when an initial chronology using ^{14}C bomb-pulse modeling has been undertaken.

There are, however, also a number of limitations when using this technique. Firstly, dampened ^{14}C activity response in the speleothem may make it difficult to estimate a precise chronology. Coupled to this is that uncertainties in the chronology are difficult to estimate, although this may be better constrained if annual/seasonal banding can be identified. In addition, any sudden or large changes in growth rates are difficult to identify, unless ^{14}C activity is highly responsive to atmospheric activity through fast SOM turnover rates. It is not clear how the SOM reservoir model would respond to a change in the SOM reservoir age over the period of study. It is certainly imperative to obtain speleothems from caves that have not had large-scale vegetation changes, such as anthropogenic land clearance, over the period of study. Finally, it could be argued that this is an expensive and time-consuming way to provide a chronology for a <100-yr-old speleothem. Although this is partially true, it is currently the only method available in many situations, and, as well as providing a basic chronology, the modeling also provides an estimate of SOM reservoir residence times, which gives us a good idea of soil carbon dynamics. If this detailed work is carried out on a speleothem that overlaps

the instrumental record, it provides a key to interpreting the longer paleoclimate records contained in other speleothems from the same cave. This is a crucial step that should be undertaken before expending further money and time analyzing older speleothems.

ACKNOWLEDGMENTS

We thank DECCW, Jenolan Caves Trust, and National Parks for permission to collect the speleothems, accommodation, and field support. The authors thank other members of the AMS group, Australian Nuclear Science and Technology Organisation (ANSTO) for helping with sample preparation and ^{14}C measurement. We gratefully acknowledge funding from the Australian Institute of Nuclear Science and Engineering (AINSE) for high-precision AMS ^{14}C measurements (Grant 06/054 and AINSTU1007), ANSTO's Cosmogenic climate Archives of the Southern Hemisphere (CcASH) Project, the Sydney Catchment Authority, and the Australian Research Council.

REFERENCES

Baker A, Smart PL, Edwards RL, Richards DA. 1993. Annual growth banding in a cave stalagmite. *Nature* 364(6437):518–20.

Baskaran M, Illiffe TM. 1993. Age determination of recent cave deposits using excess ^{210}Pb – a new technique. *Geophysical Research Letters* 20(7):603–6.

Fairchild IJ, Smith CL, Baker A, Fuller L, Spötl C, Mattey D, McDermott F, EIMF. 2006. Modification and preservation of environmental signals in speleothems. *Earth-Science Reviews* 75(1–4):105–53.

Fink D, Hotchkis M, Hua Q, Jacobsen G, Smith AM, Zoppi U, Child D, Mifsud C, van der Gaast H, Williams A, Williams M. 2004. The ANTARES AMS facility at ANSTO. *Nuclear Instruments and Methods in Physics Research B* 223–224:109–15.

Gagan MK, Chivas AR, Isdale PJ. 1994. High-resolution isotopic records from corals using ocean temperature and mass spawning chronometers. *Earth and Planetary Science Letters* 121(3–4):549–58.

Genty D, Massault M. 1997. Bomb ^{14}C recorded in laminated speleothems: calculation of dead carbon proportion. *Radiocarbon* 39(1):33–48.

Genty D, Massault M. 1999. Carbon transfer dynamics from bomb-^{14}C and $\delta^{13}C$ time series of a laminated stalagmite from SW France—modelling and comparison with other stalagmite records. *Geochimica et Cosmochimica Acta* 63(10):1537–48.

Genty D, Quinif Y. 1996. Annually laminated sequences in the internal structure of some Belgian stalagmites; importance for paleoclimatology. *Journal of Sedimentary Research* 66(1):275–88.

Genty D, Vokal B, Obelic B, Massault M. 1998. Bomb ^{14}C time history recorded in two modern stalagmites—importance for soil organic matter dynamics and bomb ^{14}C distribution over continents. *Earth and Planetary Science Letters* 160(3–4):795–809.

Genty D, Baker A, Massault M, Proctor C, Gilmour M, Pons-Branchu E, Hamelin B. 2001. Dead carbon in stalagmites: carbonate bedrock paleodissolution vs. ageing of soil organic matter. Implications for ^{13}C variations in speleothems. *Geochimica et Cosmochimica Acta* 65(20):3443–57.

Geyh MA. 2005. ^{14}C dating – still a challenge for users? *Zeitschrift für Geomorphologie Supplement* 139:63–86.

Hua Q. 2009. Radiocarbon: a chronological tool for the recent past. *Quaternary Geochronology* 4(5):378–90.

Hua Q, Barbetti M. 2004. Review of tropospheric bomb ^{14}C data for carbon cycle modeling and age calibration. *Radiocarbon* 46(3):1273–98.

Hua Q, Barbetti M, Jacobsen G, Zoppi U, Lawson EM. 2000. Bomb radiocarbon in annual tree rings from Thailand and Australia. *Nuclear Instruments and Methods in Physics Research B* 172(1–4):359–65.

Hua Q, Jacobsen GE, Zoppi U, Lawson EM, Williams AA, Smith AM, McGann MJ. 2001. Progress in radiocarbon target preparation at the ANTARES AMS Centre. *Radiocarbon* 43(2A):275–82.

Hua Q, Barbetti M, Zoppi U, Chapman DM, Thomson B. 2003. Bomb radiocarbon in tree rings from northern New South Wales, Australia: implications for dendrochronology, atmospheric transport, and air-sea exchange of CO_2. *Radiocarbon* 45(3):431–47.

Jennings JN, James JM, Montgomery NR. 1982. The development of the landscape. *Sydney Speleological Society Occasional Paper* 8:45–64.

Mattey D, Lowry D, Duffet J, Fisher R, Hodge E, Frisia S. 2008. A 53 year seasonally resolved oxygen and carbon isotope record from a modern Gibraltar speleothem: reconstructed drip water and relationship to local precipitation. *Earth and Planetary Science Letters* 269(1–2):80–95.

McDermott F. 2004. Palaeo-climate reconstruction from stable isotope variations in speleothems: a review. *Quaternary Science Reviews* 23(7–8):901–18.

McDonald J. 2005. Climate controls on trace element variability in cave drip waters and calcite: a modern study from two karst systems in SE Australia [unpublished PhD thesis]. Callaghan: The University of Newcastle.

Press WH, Teukolsky SA, Vetterling WT, Flannery BP. 2007. Minimization or maximization of functions (Chapter 10). In: *Numerical Recipes: The Art of Scientific Computing*. 3rd edition. Cambridge: Cambridge University Press. p 487–562.

Richards DA, Dorale JA. 2003. Uranium-series chronology and environmental applications of speleothems. *Uranium-Series Geochemistry* 52(1):407–60.

Roberts MS, Smart PL, Baker A.1998. Annual trace element variations in a Holocene speleothem. *Earth and Planetary Science Letters* 154(1–4):237–46.

Stuiver M, Braziunas TF. 1998. Anthropogenic and solar components of hemispheric ^{14}C. *Geophysical Research Letters* 25(3):329–32.

Tooth AF, Fairchild IJ. 2003. Soil and karst aquifer hydrological controls on the geochemical evolution of speleothem-forming drip waters, Crag Cave, southwest Ireland. *Journal of Hydrology* 273(1–4):51–68.

Trumbore SE. 1993. Comparison of carbon dynamics in tropical and temperate soils using radiocarbon measurements. *Global Biogeochemistry Cycles* 7(2):275–90.

Verdon-Kidd DC, Kiem AS. 2009. Nature and causes of protracted droughts in southeast Australia: comparison between the Federation, WWII, and Big Dry droughts. *Geophysical Research Letters* 36: L22707, doi:10.1029/2009GL041067.

Vogel JC, Marais M. 1971. Pretoria radiocarbon dates I. *Radiocarbon* 13(2):378–94.

APPENDIX

Genty and Massault (1999) presented a forward model for $\delta^{14}C$ in speleothems. The principal equation in that model describes the soil $\delta^{14}CO_2$ ($a^{14}C_g$) as a function 3 soil organic matter reservoirs:

$$a^{14}C_g = C_1(a^{14}C_{atm\text{-}Y1}) + C_2(a^{14}C_{atm\text{-}Y2}) + C_3(a^{14}C_{atm\text{-}Y3})$$

where C_1, C_2, C_3 are the reservoir mixing coefficients ($C_1 + C_2 + C_3 = 1$), and $a^{14}C_{atm\text{-}Yi}$ is the mean atmospheric activity over *Yi* years before time *t*.

The secondary equations that turn $a^{14}C_g$ into $\delta^{14}C_{sp}$ are

$$a^{14}C_{DIC0} = a^{14}C_g + 0.23(-9483/T + 23.89)$$

$$a^{14}C_{DIC} = (1-dcp/100)a^{14}C_{DIC0} \text{ (assuming } a^{14}C_{limestone} = 0)$$

$$= a^{14}C_{DIC} + 0.23(-4232/T + 15.1)$$

where *dcp* = dead carbon proportion (the difference as a % between the DIC before and after limestone dissolution), and T = temperature (K).

In this study, the latter parameters are assumed to be nearly constant over the time range of speleothem growth (<100 yr). This leaves the 6 unknown parameters above. Genty and Massault (1999) solved the model by choosing parameters that they thought would provide an approximate fit, but the method presented herein is more rigorous.